10º Congreso de Exploración y Desarrollo de Hidrocarburos
Simposio de Geofísica: La Geofísica como vínculo entre el conocimiento de la tierra y la sociedad

THIN LAYER DETECTION AND CHARACTERIZATION USING FREQUENCY-ENHANCED SEISMIC DATA AND SIMULTANEOUS INVERSION: COMODORO RIVADAVIA FORMATION, GOLFO SAN JORGE BASIN, ARGENTINA

Gisela Porfiri[1], John Castagna[2], Augusto F. Brennan[3], Luis A. Vernengo[3]

1: DataSeismic Corporation, gporfiri@dataseismic.com

2: University of Houston, jpcastagna@uh.edu

3: Panamerican Energy, abrennan@pan-energy.com, lvernengo@pan-energy.com

Palabras clave: **alta frecuencia, Vp/Vs, impedancia acústica, inversión simultanea**

RESUMEN

Detección y caracterización de capas delgadas usando datos sísmicos de alta frecuencia e inversión simultánea: Formación Comodoro Rivadavia, Cuenca del Golfo San Jorge, Argentina.

El objetivo de este trabajo es identificar, interpretar y caracterizar las capas delgadas dentro de los depósitos basales de la Formación Comodoro Rivadavia (Cretácico). Para esto se utilizaron las más modernas tecnologías como son el proceso de aumento de frecuencia y el de inversión simultánea de los datos sísmicos pre-stack.

Estas capas de bajo espesor (~10 m) que en general están saturadas de gas, no son completamente resueltas por los datos sísmicos convencionales por lo cual se dificulta la generación de mapas confiables que predigan su espesor y ubicación más allá de los datos de pozo.

A partir de la identificación de los intervalos delgados de interés en los pozos existentes se intentó identificar y mapear el tope y base de los mismos combinando los datos sísmicos de alta frecuencia y los resultados de la inversión simultánea.

Como resultado de este trabajo, se logró resolver el tope y la base de los intervalos de interés (antes por debajo de la resolución sísmica) y caracterizar la respuesta geofísica de los mismos utilizando los volúmenes de impedancia acústica y relación Vp/Vs.

INTRODUCTION

The San Jorge Basin has been and is still being explored for hydrocarbon production. With the vast knowledge of the basin and new technologies we can now explore thin hydrocarbon bearing layers previously ignored. This study focused on the thin sand layers within Comodoro Rivadavia basal deposits unofficially known as Tobaceous Section. This interval is composed by tobaceous sandstones and sandy tuffs with shale intervals intercalations which act as seals. These rocks correspond to sediments deposited on a fluvial paleo-environment characterized by the presence of volcanic ash.

The main objective are several thin layers identified on well data with thicknesses below 10 meters which are not resolved in the available seismic data.

The challenge of this work is to apply the sparse-layer reflectivity inversion technique (Zhang and Castagna, 2011) to increase seismic resolution, show the reliability and stability of the results, and use this high-frequency seismic data along with P-impedance and Vp/Vs volumes from simultaneous inversion process to detect, identify, and map the productive thin layers for future well planning.

HIGH RESOLUTION SEISMIC DATA

Sparse-layer reflectivity inversion technique described by Zhang and Castagna (2011) was applied to the approximately 40 km2 of pre-stack seismic data to increase the data frequency content. Said method uses a priori information and spectral decomposition to improve the resolution, but does not directly utilize well logs in a starting model. Thin beds below tuning thickness (i.e. maximum constructive interference that occurs when the bed thickness reaches one quarter of the wavelength at dominant frequency (Kallweit and Wood, 1982; Brown, 2004)) can be imaged by inverting the frequency spectra for layer thickness using complex spectral analysis.

The first step in this process is to improve the signal-to-noise ratio of the input gathers by applying a conditioning sequence specifically designed to suppress coherent and random noise (figure 1) while maintaining the amplitude anomalies and AVO gradient. For this particular set of gathers, the conditioning sequence included the application of a time variant filter, angle mute at 45 degree angle of incidence, offset to angle conversion (using velocities), multiple removal, and creating partial stacks which will be the input for the sparse-layer reflectivity inversion process. As shown in figure 2, the signal-to-noise ratio has been improved after conditioning and the resulting image displays more defined reflectors.

Frequency-enhanced seismic data was produced using conditioned partial stacks as the input. The resulting higher frequency gathers doubled the central frequency, which was improved from 25 to 40 Hz (Figure 3). As mentioned before, quality control (qualitative and quantitative) of the enhanced-frequency results are key to understand and interpret the high resolution seismic data. First, confidence must be built based on how well the image conforms to geological expectations (Zhang and Castagna, 2011), paying attention to the continuity of the reflectors, the structural consistency with the input, and the overall signal-to-noise ratio. Then, well to seismic ties and AVO gradient must be analyzed for consistency with the input data.

The synthetic seismogram ties to the seismic trace generate the depth-time relationship between the seismic and well data. Two key wells were used to compare the correlation and the goodness of fit between the well vs. conditioned and frequency-enhanced seismic data respectively (Figure 4 and 5). It is important to remark that the time-depth relationships are defined with the

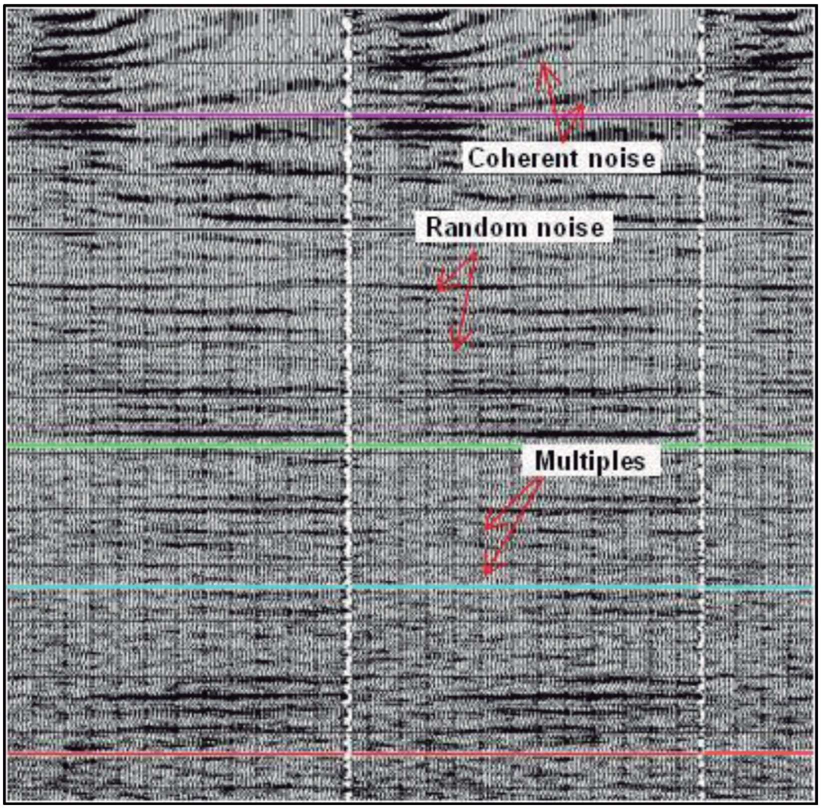

Figure 1. Input pre-stack data. The gathers displayed along the inline represent raw data that will be conditioning in order to suppress multiple events, random and coherent noise, etc.

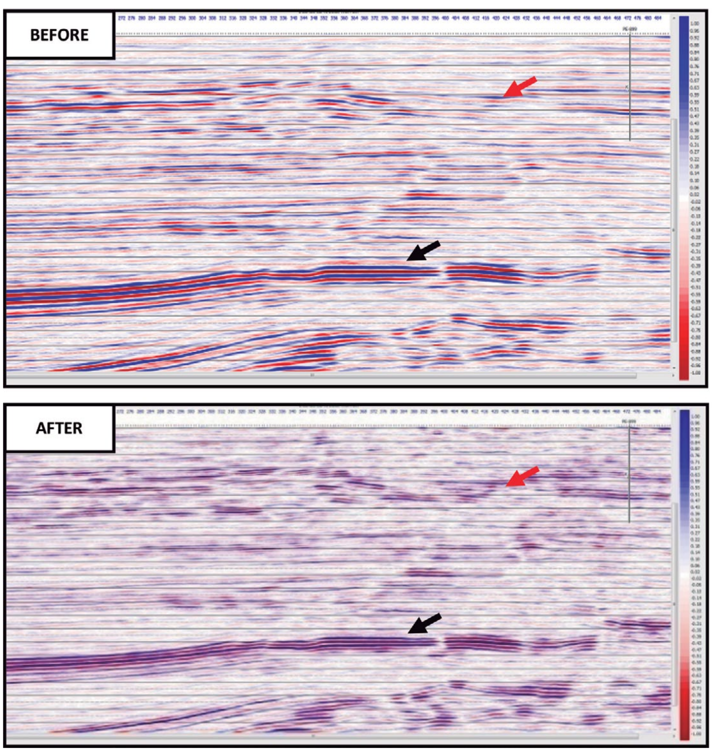

Figure 2. Before and after gather conditioning. The upper image displays the full stack before conditioning. Multiples and random noise can be observed. The lower image displays the full stack of conditioned gathers where multiples (black arrow) are attenuated and/or removed. Also, the shallow section shows more detail and reflector continuity after noise removal.

well ties to the input full stacked data and remained intact when comparing the well synthetic to the frequency-enhanced full stacked data. The wavelets used for synthetic seismogram generation are extracted from the stacked input and frequency-enhanced seismic data, respectively. All wells show a good correlation with the frequency-enhanced seismic data, with a centered cross correlation coefficient consistent with the zero phase input data. It is observed that the cross-

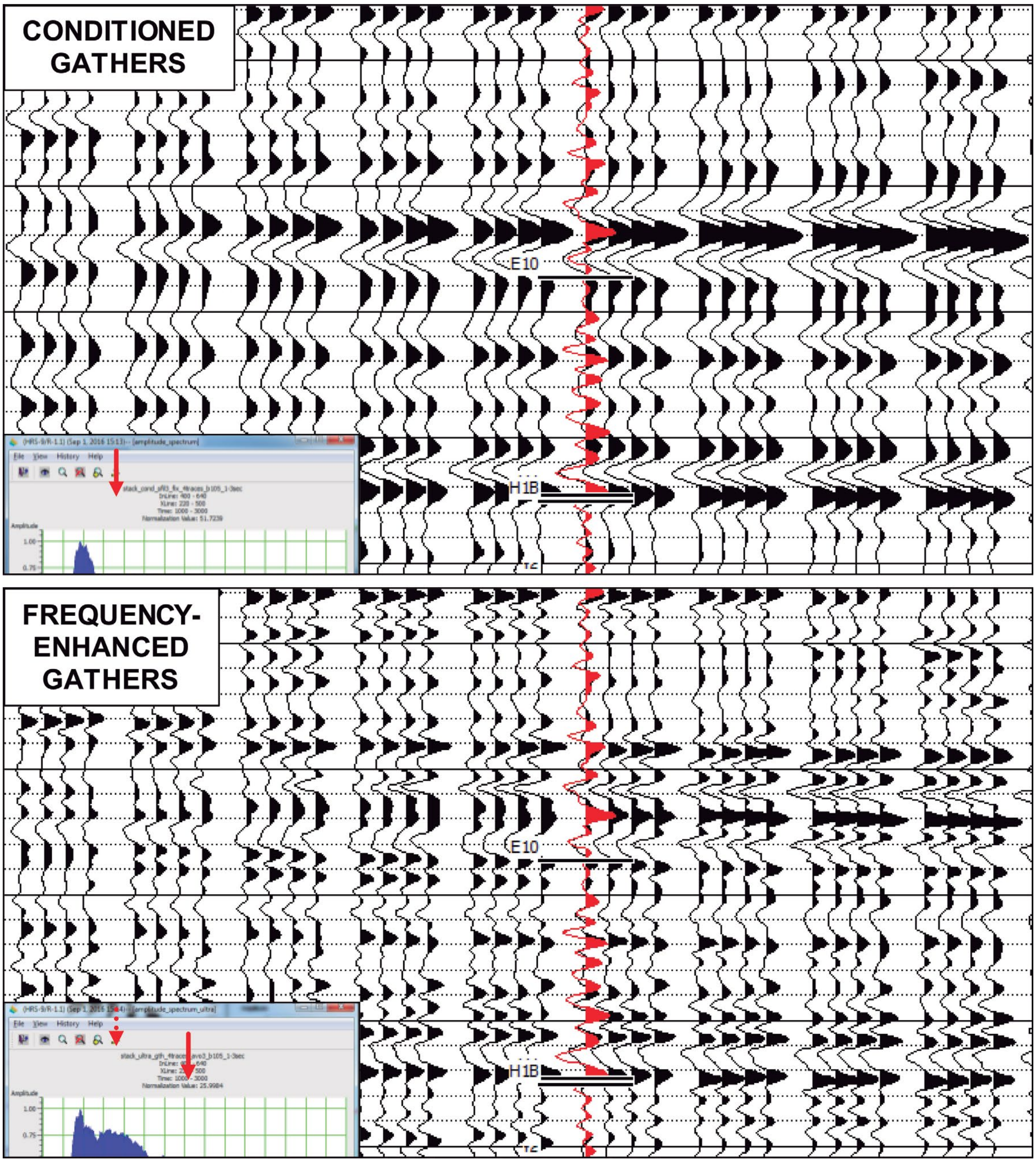

Figure 3. Input gathers vs. frequency-enhanced gathers. It is noticeable the increased level of detail and resolution on the frequency-enhanced data. The red trace represents the well's synthetic seismogram at the frequency-enhanced data frequency, and shows a very good correlation with this results. The amplitude vs. frequency spectrum charts show the resulting frequency is twice as the input.

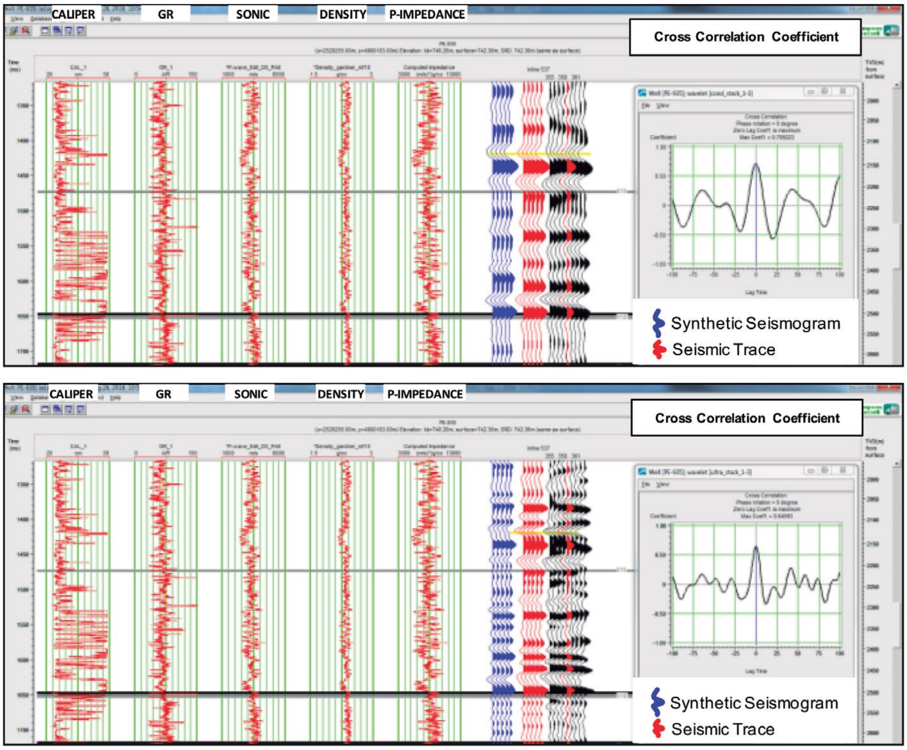

Figure 4. Well to seismic tie at P-935 well. The correlation between the extracted trace (red) and the synthetic seismogram (blue) shows a good fit and consistency with both conditioned (upper image) and frequency-enhanced data (lower image).

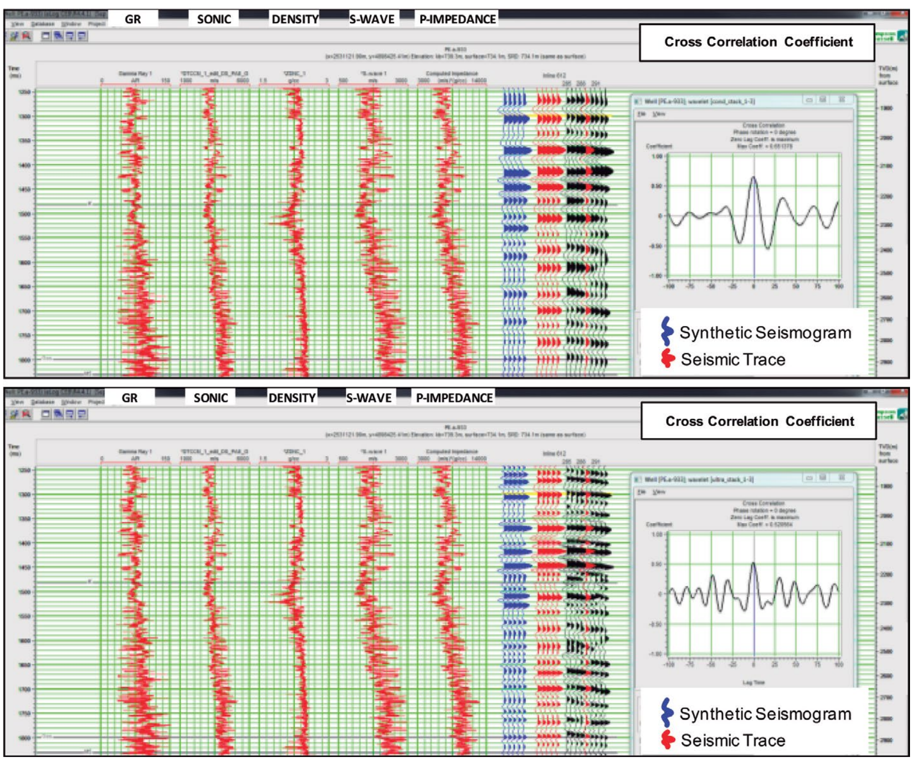

Figure 5. Well to seismic tie at P-933 well. The correlation between the extracted trace (red) and the synthetic seismogram (blue) shows a good fit and consistency with both conditioned (upper image) and frequency-enhanced data (lower image).

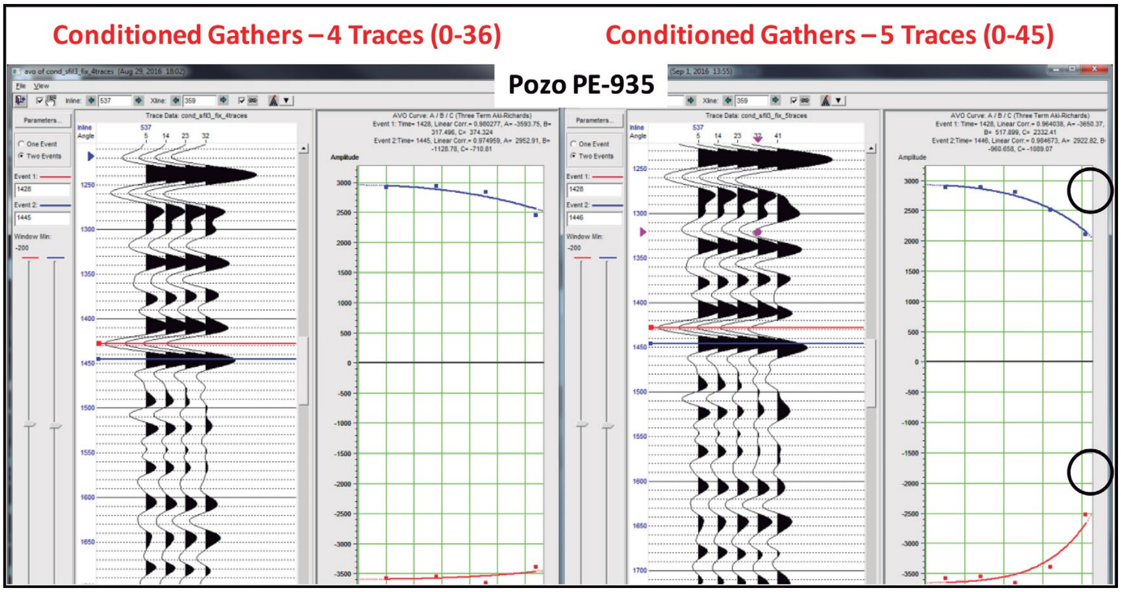

Figure 6. AVO Gradient Analysis shows that the further offset of the conditioned gathers is out of trend.

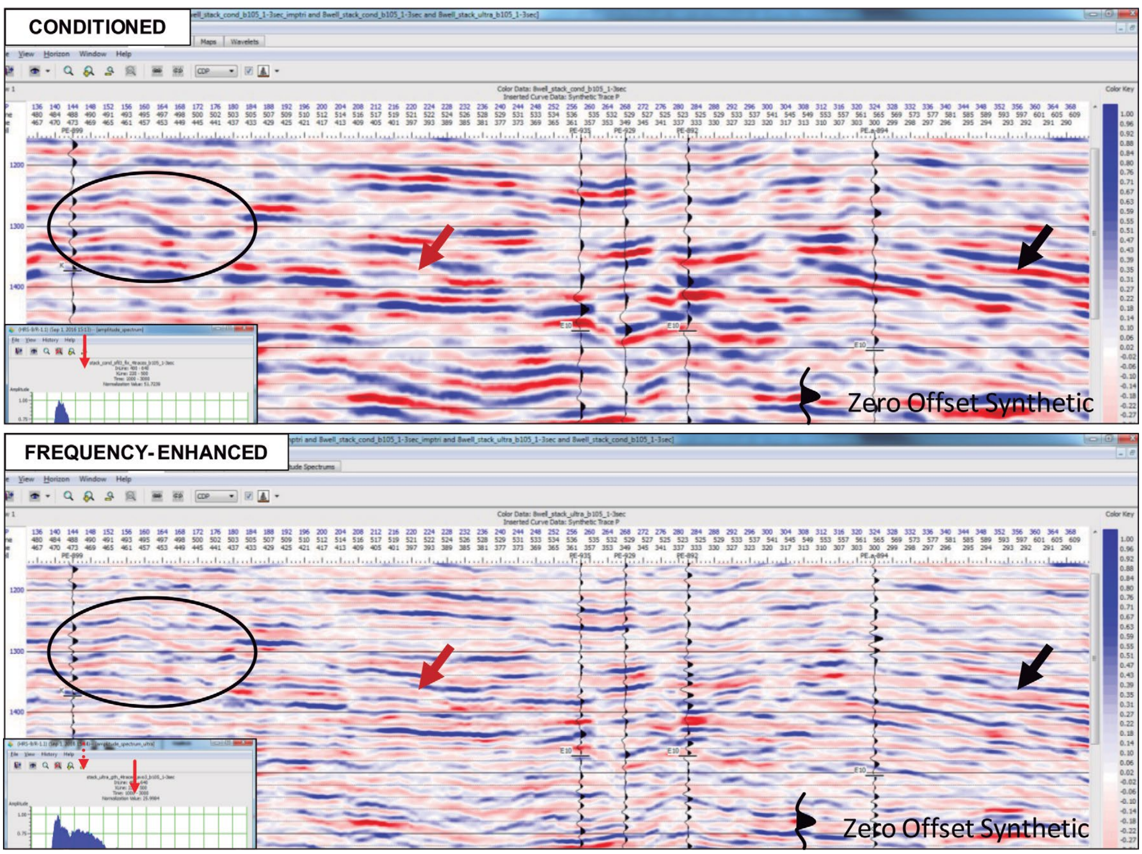

Figure 7. Conditioned vs. Frequency-enhanced full stacks. The frequency-enhanced data shows an increased level of detail by defining wedge closures (red arrows) and internal geometry (black arrows and circle).

correlation coefficient of the well to frequency-enhanced seismic data tie decreases, this is due to minimum time shifts that in higher frequency data can impact the error calculation.

Since the next step is to simultaneously invert the frequency-enhanced seismic gathers, the AVO gradient must be analyzed for consistency with the input gathers. The most prominent reflectors along the target time interval are analyzed in the key wells. Figure 6 illustrates the consistency of the AVO gradient for the input vs. conditioned gathers for the partial stacks (0-45 degree angle of incidence). The analysis shows that the further offset of the conditioned data is out of trend. This can be the result of lower signal to noise ratio of the further offset input data, which makes the results less stable. Hence, the far offset trace was removed from the final conditioned data results and will not be taken as an input neither for the frequency-enhance nor simultaneous inversion processes. Finally, the comparison of the conditioned vs. frequency-enhanced stacked data (figure 7) shows an improved image of geological features and structural consistency between both datasets .

As evidenced by all the quality control processes, frequency-enhanced data is reliable and will be use as a practical tool for seismic exploration and reservoir characterization purposes. The best example is illustrated in figure 9, where the thin layers (~ 3-10 m) of the well P-933 are detected and in some cases resolved.

SIMULTANEOUS INVERSION

The objective of this work comprises simultaneous inversion of the original and the frequency-enhanced seismic data (best case scenario for each dataset). Then compare the volumes at the levels of interest and study any resolution improvement.

Simultaneous inversion is one of the pre-stack seismic inversion processes in which lithologic volumes (P-impedance, S-impedance, and density) are created simultaneously. The method is based in three assumptions: 1) linearized approximation for reflectivity holds, 2) the Aki-Richards equation gives the reflectivity as a function of angle, and 3) there is, to first order, a linear relationship between Pimpedance and both S-impedance and density (Gardner's relationship: $\Delta\delta/\delta=(1/4)(\Delta Vp/Vp)$, and Castagna's equation: $Vs=(Vp-1360)/1.16$). HampsonRussell software uses the AVO Equation (Fatti *et al.* 1994) that considers the P-reflectivity, S-reflectivity, a geometric factor (that includes the different incidence angles of the gather), and density reflectivity (Hampson and Russell, 2005).

Since the seismic input is band-limited, i.e. it has low and high cutoffs in the frequency spectra; The absolute impedance variations can be calculated by adding the missing low-frequencies using a priori information (well logs and interpreted horizons) to build P-Impedance, S-Impedance and density initial low-frequency models. In this case, the low frequency model was built by propagating well log properties from well to well along interpreted horizons, with a maximum frequency of 15 Hz.

The resulting absolute P and S-impedance, and Vp/Vs volumes from the frequency-enhanced data showed much more detail and defined layers when compared to the input results. Figure 8 shows an arbitrary line across the key wells, the calculated acoustic and elastic properties at the wells are filtered to the frequency-enhanced data frequency content. While well to inverted volumes correlation is very high, the absolute values do not always compare. This is usually the case when well logs are not normalized from well to well (due to different acquisition tools, dates, etc), and more petrophysical analysis is needed to create a more robust low frequency model. Since the main objective of this work is to improve detection and mapping of productive thin layers, the relative component (i.e. the low frequency model contribution will be removed) of the inversion results will be used. Therefore, we can focus of property contrast instead of absolute value matching.

The main objective is to identify and map the 3 to 10 m thick gas layers penetrated by P-933 well, which is the only deep well in the area. These layers are characterized by relative higher P-Impedance and low Vp/Vs values (Figure 9). The M13 layer is the main objective because

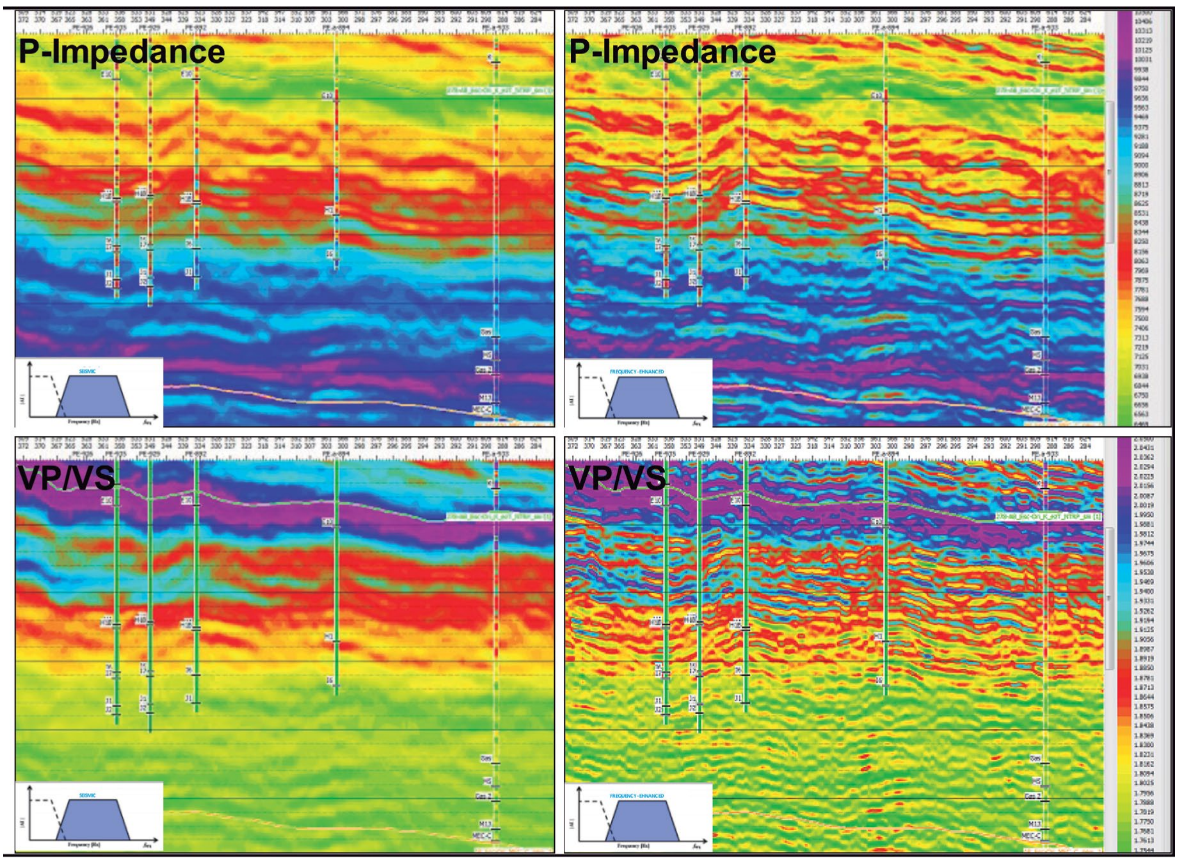

Figure 8. Comparison between simultaneous inversion results from the conditioned vs. frequency-enhanced gathers. The overall distribution of the attribute values is consistent between conditioned and frequency-enhanced data. The comparison shows not only that a greater level of detail is observed on the higher frequency P-Impedance and Vp/Vs results, but a high correlation with the attribute values at the well (the Vp/Vs could only be calculated at one well with recorded s-wave log).

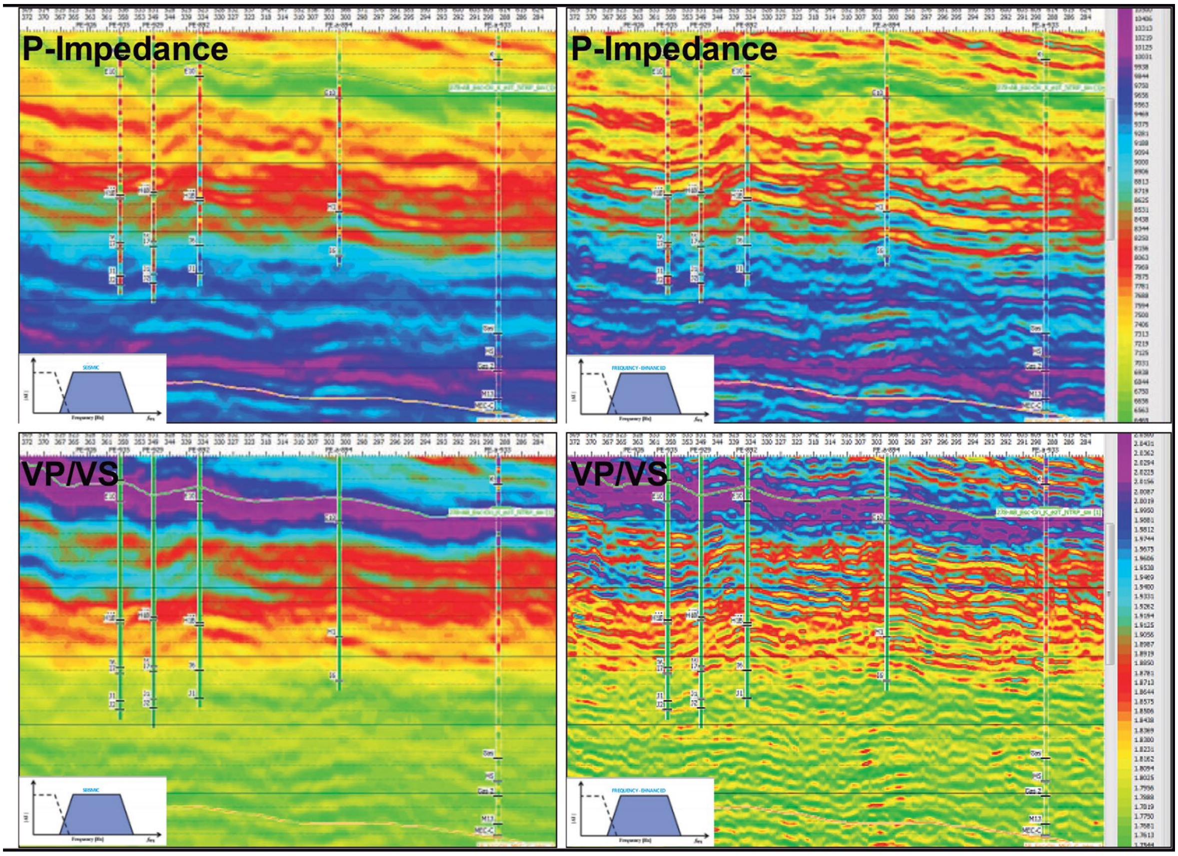

Figure 9. P-933 well log display shows that the thin layers of interest are characterized by relatively higher P-Impedance and low Vp/Vs values. It is also noticeable the increased resolution that allows to detect top and base of the thin layers (black boxes and arrow).

proper mapping of this layer is needed for future well planning. Hence, the P-Impedance and Vp/Vs relative attributes are used for the interpretation. As shown in figure 10, M13 can be hardly interpreted away from the well when using the input seismic data inversion results. A higher impedance interval is defined and can be interpreted. However, the same attribute resulting from the frequency-enhanced data results shows that this layer is actually subdivided and the higher impedance zone is in a slightly shallower position than the previous interpretation. The same happened when using Vp/Vs attribute, the layer is much more defined with frequency-enhanced data results and helps in interpreting the shallower anomaly for the M13 layer. For this layer, the use of more than one attribute is critical for an accurate interpretation aiding in proper well planning and landing point definition.

CONSLUSIONS

Frequency-enhanced seismic data has been proven as a valuable tool in detecting and interpreting seismically thin gas layers. The extensive quality control processes applied showed the

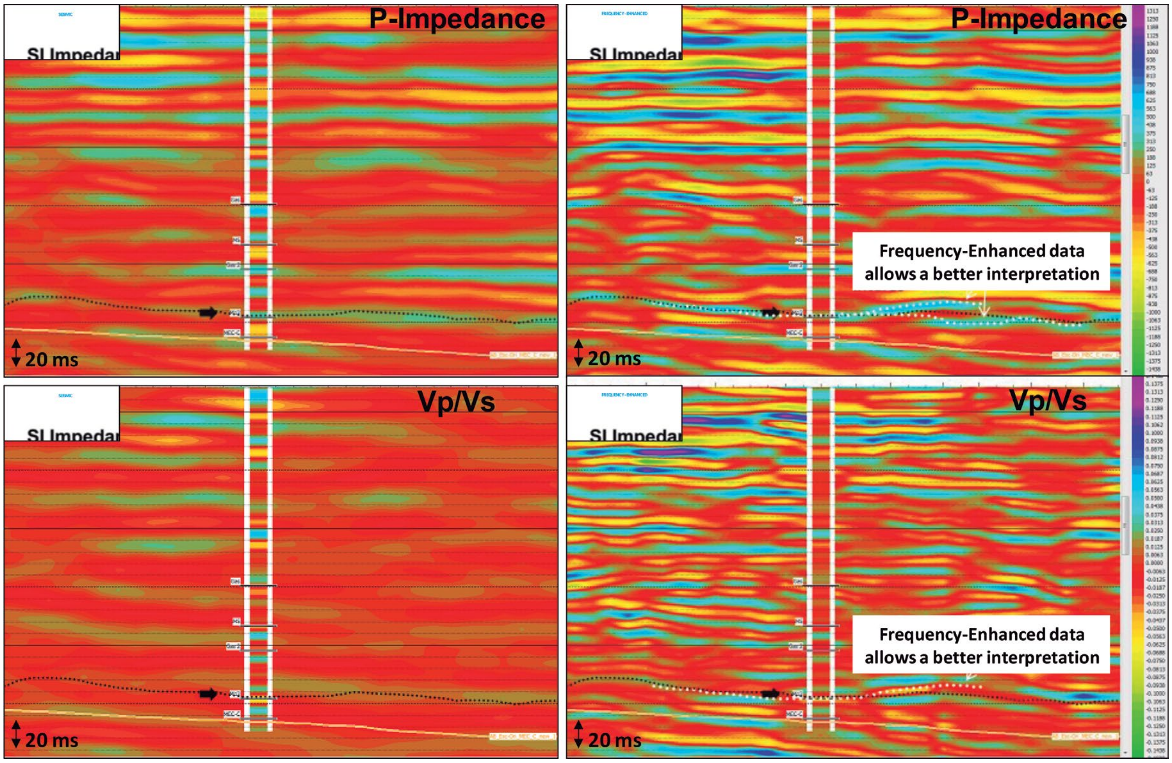

Figure 10. Relative P-Impedance and Vp/Vs attributes from conditioned vs. frequency-enhanced data. This image shows how the interpretation of the M 13 layer was improved by using higher frequency data results. The original higher P-Impedance/low Vp/Vs value horizon (black dotted line) interpreted on the lower frequency data is barely seen, but with addition of the higher-frequency results it can be tracked down along the IL (white dotted line). Looking at the relative higher frequency P-Impedance the previously interpreted horizon seems to divide in two higher P-Impedance zones. When analyzing that on the relative higher frequency Vp/Vs the lower values of the previously interpreted horizon are defined in a single interval. This is a very important aspect that shows that the combination of more than one attributes allowed a better horizon placement.

reliability of the frequency-enhanced data. Well to seismic ties not only showed excellent quality correlation but also consistency when compared to the input seismic data.

Simultaneous inversion results aided in the interpretation of the interval of interest at the P-933 well. The combination of P-Impedance and Vp/Vs attributes allowed a more accurate interpretation of the M13 layer.

We conclude that frequency-enhanced seismic data inversion may allow better definition of productive zones for future area development and well planning.

REFERENCES

Brown, A. R., 2004, Interpretation of Three-dimensional Seismic Data, 6th edition: AAPG Memoir 42.

Fatti J.,G. Smith, P. Vail, P. Strauss, and P. Levitt, 1994, Detection of gas in sandstone reservoirs using AVO analysis: A 3D seismic case history using the Geostack technique: Geophysics, 59, 1362-1376.

Hampson, D. P., B. H. Russell, and B. Bankhead, 2005, Simultaneous inversion of pre-stack seismic data. 75th Annual International Meeting, SEG, Expanded Abstracts, 1633-1637.

Kallweit, R. S., and L. C. Wood, 1982, The limits of resolution of zero-phase wavelets: Geophysics, 47, no.7, 1035–1046.

Zhang, R., and Castagna, J. P., 2011, Seismic sparse-layer reflectivity inversion using basis pursuit decomposition: Geophysics, 76, no.6, R147–R158.

10° CONGRESO DE
EXPLORACIÓN Y
DESARROLLO DE
HIDROCARBUROS

Energía y Sociedad
aliados inseparables
Mendoza 2018